ON THE SOFT ORIGAMI ROBOTS WITH SHAPE MEMORY ALLOYS ARTIFICIAL MUSCLES

LIGIA MUNTEANU[1], VETURIA CHIROIU[1], CORNEL BRIŞAN[2], CRISTIAN RUGINĂ[1], VALERICA MOŞNEGUŢU[1]

Abstract. Folding in nature allows development of complex structures such as flowers, insect wings, proteins and intestines. The origami robots can be obtained from folding the elastomer foils and by embedding the shape memory alloys (SMAs) elements. The SMA artificial muscles have the role of producing the fast motion. The hardening effect corresponding to the smooth hysteretic behaviour of SMA artificial muscle is investigated together to the actuation and the force performance by using a Bouc-Wen model coupled to the intrinsic time which governs the behavior of the SMAs. The soft robots can offer a good opportunity for drug delivery and minimally-invasive surgical procedures.

Key words: Origami soft robots, Shape memory alloys (SMA), Bouc-Wen model, Surgery.

1. INTRODUCTION

During the last two decades, the research on the robots made of soft materials with similar elasticity as biological materials has focused to the elastic deformation and fast motion when submitted to overload/impacts and to the shape adaptation to the external constraints and obstacles [1, 2].

Bio-inspired systems which mimic the capabilities of insects or animals, have suggested the architecture not only for the rigid bodies but also to the elastic elements associated with the soft parts [3]. The inspiration of these robots came from observing the waves of the snake movement and the enhanced motions given by changing the waves phases and amplitudes.

The robot considered in this paper is 3 mm in diameter and 31.5 mm long, consisting of 15 revolute joints of 0.5 mm each. The joints are perpendicular to each other in order to achieve different configurations. The 15 SMA muscles with cylindrical forms of length 1.5mm are placed between joints. Taking inspiration from the Japanese art of folding technique [4–8], the robot is obtained by folding

[1] Insitute of Solid Mechanics of the Romanian Academy, Bucharest, Romania
[2] Technical University of Cluj-Napoca, Cluj-Napoca, Romania

an elastomer foil and inserting the SMA elements to mimic muscles. The scheme of this robot is presented in Fig. 1.

The robot shown in Fig. 1 contains more identical structures like a bird-neck mechanism. Similar works regarding the soft robots obtained by folding can be found in [9−11].

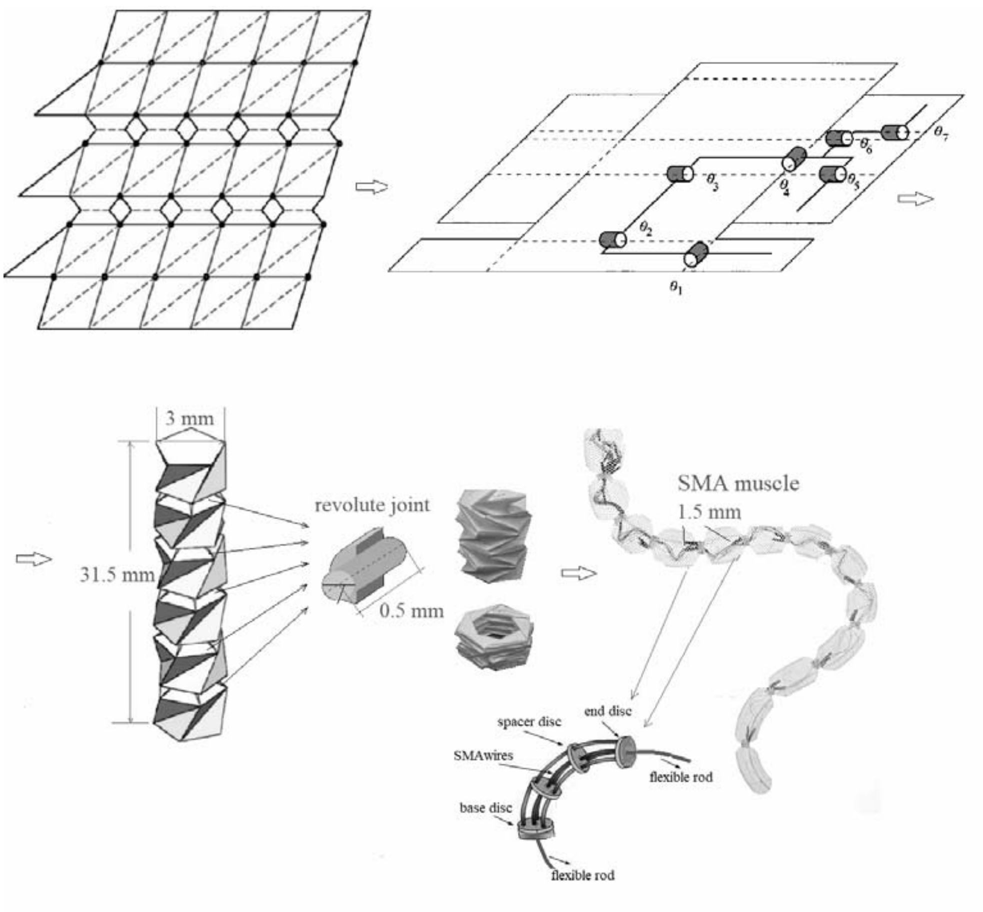

Fig. 1 – Scheme of the robot obtained by folding the elastomer foil.

The paper is not including the embedding of other electronics or energy sources. As a solution for muscle-like actuators, the shape memory alloys (SMA) are chosen due to their transitions in the material structure under temperature changes which allow the recovery of stored elastic energy [12]. The SMAs have the advantage of a large force/weight ratio extended to the micron size [13, 14]. The SMA artificial muscles are characterized by the motion of the robot in flexion. The relationship between the bending angle and the actuation is investigated.

2. MODEL

To describe only one component of the robot, the Stewart platform is used in the form of the cable-suspended platform [15–18]. The first platform is the elastic element and the second one the cable actuation. The platforms are equilateral triangles and each cable links a node from the lower platform to the corresponding node of the upper platform [18]. An elastic central column is added to assure the platform stability. The platform exhibits 3 DOF. The joints between the column and the platforms are fixed.

In the spherical coordinates system, the generalized coordinates are defined as: h the height of the central column, the anti-clockwise angle θ starting from the positive x – axis in the (x, y) plane, the angle ϕ between the upper platform plane and the projection d of the central column in (x, y) plane. The central column bends under a circular arc of radius of curvature R.

The model of bending geometry is shown in Fig. 2, where O_1 and O_2 are the origins of the coordinates systems attached to the base and upper platform, respectively.

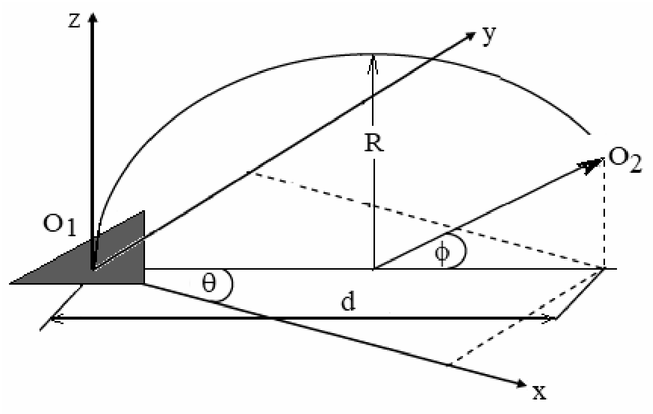

Fig. 2 – The model of bending geometry.

Only the rotations α and β about x – and y – axes, respectively, are taken into account and determined as

$$\alpha = \tan^{-1}\left(\frac{\tan\phi}{\sin\theta}\right), \ \beta = \tan^{-1}\left(\frac{\tan\phi}{\cos\theta}\right). \tag{1}$$

The nodes where the cables are attached to the base and the upper platforms are noted by A_i, and $B_i, i = 1,2,3$, respectively.

The lengths of the cables are computed as

$$l_1 = \| A_1 B_1 \| =$$
$$= \left([r \sin\alpha \sin\beta + x]^2 + [r\cos\alpha - r + y]^2 + [r\sin\alpha\cos\beta + z]^2 \right)^{1/2},$$

$$l_2 = \| A_2 B_2 \| =$$
$$= ([-r\sqrt{2}/2 + r\sqrt{2}/2\cos\beta - r/2\sin\alpha\sin\beta + x]^2 +$$
$$+[r/2 - r/2\cos\alpha + y]^2 + [z - r\sqrt{2}/2\sin\beta - r/2\sin\alpha\cos\beta]^2)^{1/2}, \quad (2)$$

$$l_3 = \| A_3 B_3 \| =$$
$$= ([-r\sqrt{2}/2 + r\sqrt{2}/2\cos\beta - r/2\sin\alpha\sin\beta + x]^2 +$$
$$+[r/2 - r/2\cos\alpha + y]^2 + [-r\sqrt{2}/2\sin\beta - r/2\sin\alpha\cos\beta + z]^2)^{1/2}.$$

3. SMA ARTIFICIAL MUSCLES

The origami robots contain the embeded artificial muscles made from shape memory alloys. The structure of the SMA muscle is shown in Fig. 3.

It consists of 4 SMA wires, a base disc with a SMA guide, an end disc, 15 spacer discs and 2 flexible rods made from steel. All discs are made of resin.

Electrical current flows into SMA wires via lead wires located in the SMA guide box in the base disc. Two types of SMA wiring arrangements are used to generate the movement. These arrangements the spacer discs must be able to generate enough force and movement to rotate the joints. Different combinations of these modes A and B can be created by variations of distances and angles. The propulsion mechanism that generates the muscle action and thus the robot's movement is achieved through a succession of combinations A and B suggested by the task of the robot. The SMA guide box controls the temperature in relation to an internal measure of time specific to SMA wires. This box is made from silicone rubber.

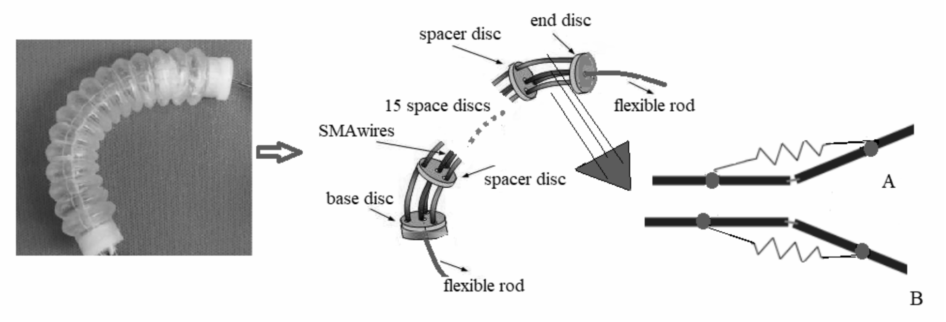

Fig. 3 – Structure of the SMA actuator.

SMA wires have the diameter 0.3 mm and the Ni content 55.4%. When electrical current flows into SMA wires, they are compressed to the length of the memorized shape and when the electrical current is turned off, the SMA wires are extended by natural cooling. The hardening effect corresponding to the smooth hysteretic behaviour of SMA artificial muscle and the investigation of the actuation and the force performance are done by using a Bouc-Wen model.

The SMA guide box controls the temperature of the wires with respect to an intrinsic time measure ϑ for muscle actuation. This measure is introduced as a non-decreasing function which depends on the strain tensor ε. It can be expressed as $\mathrm{d}\vartheta = (\mathrm{d}\varepsilon : \mathrm{d}\varepsilon)^{1/2}$, where the double dot product of two tensors is noted by ":", $A : B = \delta_{il}\delta_{jk}A_{ij}B_{kl}$, $\delta_{ij} = 1$ for $i = j$ and $\delta_{ij} = 0$ for $i \neq j$.

For $p = I$, we have $\mathrm{d}\vartheta = \| \mathrm{d}\varepsilon \|$, [19–21].

We suppose that the Helmholtz free energy density Ψ depends on a single internal variable tensor χ.

$$\begin{aligned}\Psi = (C_0/2)\mathrm{tr}(\varepsilon)^2 + (C_2/2)\varepsilon_d : \varepsilon_d + B_0\mathrm{tr}(\varepsilon)\mathrm{tr}(\chi) + \\ + B_2\varepsilon_d : \chi_d + (D_0/2)\,\mathrm{tr}(\chi)^2 + (D_2/2)\,\chi_d : \chi_d,\end{aligned} \tag{3}$$

where $\varepsilon_d = \varepsilon - 1/3\,\mathrm{tr}(\varepsilon)I$ and $\chi_d = \chi - 1/3\,\mathrm{tr}(\chi)I$ are the deviatoric parts of the strain tensor ε and of the internal variable tensor χ, respectively, I is the unit tensor. The state equation $\sigma = \dfrac{\partial\Psi}{\partial\varepsilon}$, where σ is the stress tensor, leads to

$$\sigma = (1/3)\mathrm{tr}(\sigma)I + \sigma_d = \left(C_0\mathrm{tr}(\varepsilon) + B_0\mathrm{tr}(\chi)\right)I + C_2\varepsilon_d + B_2\chi_d, \tag{4}$$

where σ_d is the deviatoric part of the stress tensor. The thermodynamic force $\tau = \dfrac{\partial\Psi}{\partial\chi}$ associated to the internal variable tensor χ becomes

$$\tau = (1/3)\,\mathrm{tr}(\tau)I + \tau_d = \left(B_0\mathrm{tr}(\varepsilon) + D_0\mathrm{tr}(\chi)\right)I + B_2\varepsilon_d + D_2\chi_d, \tag{5}$$

where τ_d is the deviatoric part of the thermodynamic force, and $\mathrm{tr}(\tau) = 3B_0\mathrm{tr}(\varepsilon)$ is the elastic hydrostatic response. From (5) we get

$$\tau_d = B_2\varepsilon_d + D_2\chi_d. \tag{6}$$

The solution of (6) is given by

$$\tau_d = B_2\int_0^{\vartheta}\exp\left(-\frac{D_2}{b_2}(\vartheta - \vartheta'\right)\frac{\partial\varepsilon_d(\vartheta')}{\partial\vartheta'}\mathrm{d}\vartheta', \tag{7}$$

for $\tau_d(0)=0$. By substituting (6), (7) into (4) we obtain

$$\sigma_d = \left(C_2 - \frac{B_2^2}{D_2}\right)\varepsilon_d + \frac{B_2}{D_2}\tau_d = \\ = \left(C_2 - \frac{B_2^2}{D_2}\right)\varepsilon_d + \frac{B_2^2}{D_2}\int_0^{\vartheta}\exp\left(-\frac{D_2}{b_2}(\vartheta-\vartheta'\right)\frac{\partial\varepsilon_d(\vartheta')}{\partial\vartheta'}\mathrm{d}\vartheta', \quad (8)$$

where $C_2 - \dfrac{B_2^2}{D_2} \ge 0$, $\dfrac{B_2^2}{D_2} > 0$. The term $\left(C_2 - \dfrac{B_2^2}{D_2}\right)\varepsilon_d$ describes the hardening effect while the integral corresponds to a smooth hysteretic behaviour.

By denoting $A_0 = C_2 - \dfrac{B_2^2}{D_2}$, $A = \dfrac{B_2^2}{D_2}$, $\beta = \dfrac{D_2}{b_2}$ and $\mu(\vartheta) = A\exp(-\beta\vartheta)$, equations (8) becomes

$$\sigma_d = A_0\varepsilon_d + \frac{B_2}{D_2}\tau_d = A_0\varepsilon_d + \int_0^{\vartheta}\mu(\vartheta-\vartheta')\frac{\partial\varepsilon_d(\vartheta')}{\partial\vartheta'}\mathrm{d}\vartheta'. \quad (9)$$

By denoting

$$z = \int_0^{\vartheta}\mu(\vartheta-\vartheta')\frac{\partial\varepsilon_d(\vartheta')}{\partial\vartheta'}\mathrm{d}\vartheta', \quad (10)$$

equations (9) and (10) become

$$\sigma_d = A_0\varepsilon_d + z,\ \mathrm{d}z = A\mathrm{d}\varepsilon_d - \beta z\,\mathrm{d}\vartheta. \quad (11)$$

We recognize in (11) the hysteretis model proposed by Bouc [19, 21] in the differential form

$$w(t) = A_0 u(t) + z(t),\ \mathrm{d}z = A\mathrm{d}u - \beta z\,\mathrm{d}\vartheta, \quad (12)$$

with $u(t)$ and $w(t)$ are the input and output time-dependent functions, and $A_0 \ge 0$. The function $z(t)$ describes the time history of the input variable u which can be the actuation or the force. The hereditary kernel $\mu(\vartheta-\vartheta') \ge 0$ has an exponential form

$$\mu(\vartheta) = A\exp(-\beta\vartheta),\ A,\beta > 0. \quad (13)$$

1The time function ϑ represents the total variation of u.

4. RESULTS

The lengths of cables are computed with (2). The desired positions of the upper platform are obtained next. The lengths of the cables for six configurations of the upper platform are shown in Fig. 4. The curvature of the central elastic column follows a circular arc within this 30° angular deformation.

The actuation performance is analyzed by studying the relationship between the bending of the robot and the actuation. The maximum displacement for different times is investigated.

The relationship between the maximum displacement of the SMA muscle and the angle is shown in Fig. 5. The vertical axis represents displacement and the horizontal axis, the time. The displacement is 3 mm for a bending of 90 degrees.

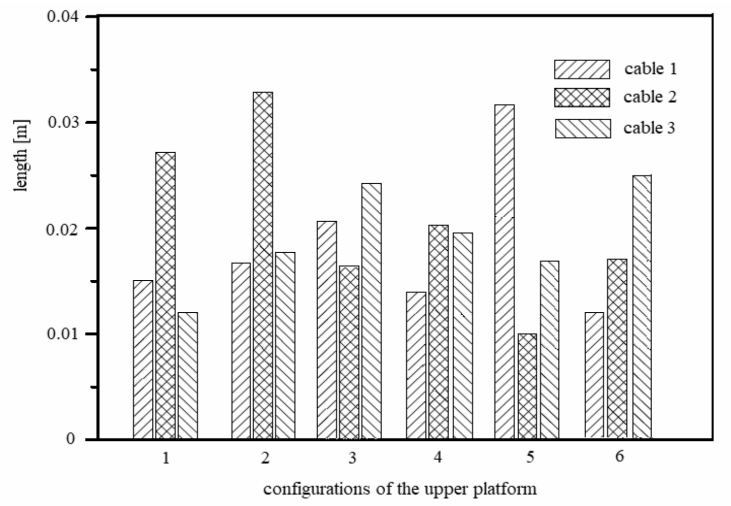

Fig. 4 – The lengths of cables for different configurations.

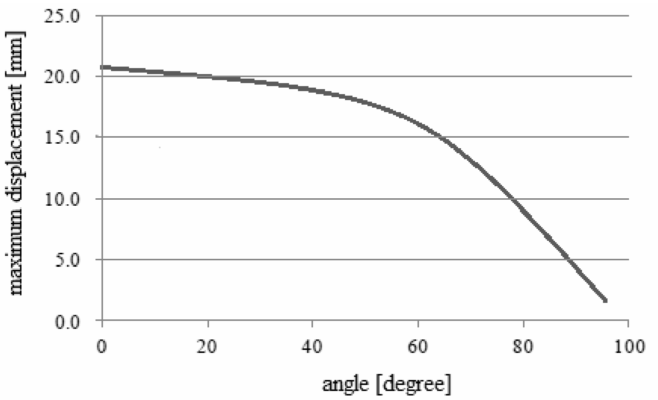

Fig. 5 – The relationship between the maximum displacement of the SMA actuator and the angle.

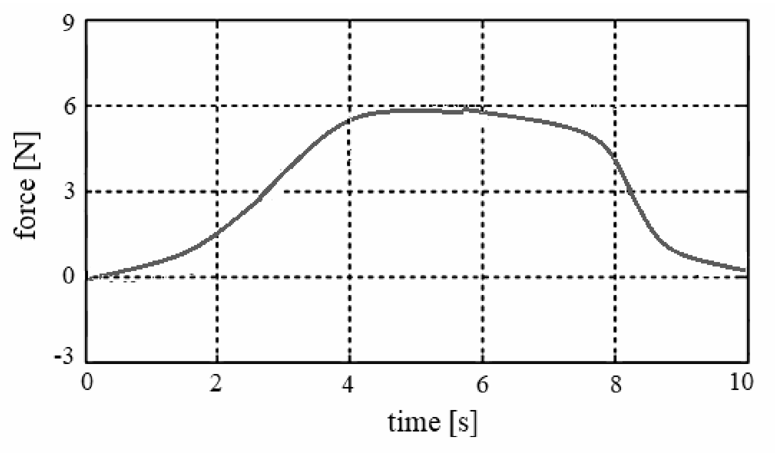

Fig. 6 – Force calculation during activation.

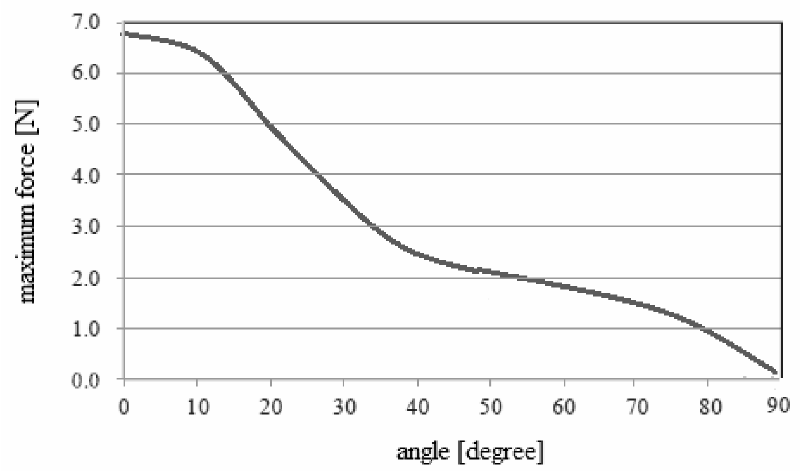

Fig. 7 – The relationship between the maximum force and the angle.

The variation of the force with respect to time during activation is shown in Fig. 6. The maximum force and the relationship between the bended robot and the force of the actuator is also investigated. The bending angle varies continuously from 0 to 90 degrees. Simulations showed that the SMA muscles can generate forces as high as 10 N. The relationship between the maximum force and the angle is shown in Fig. 7.

After several loading/unloading paths, Fig. 8 shows the progressive enhancement of the stiffness (red lines). The explanation consists in the phase transformation of the SMA material. The martensitic variants are nucleating in response to the direction of the moving [19].

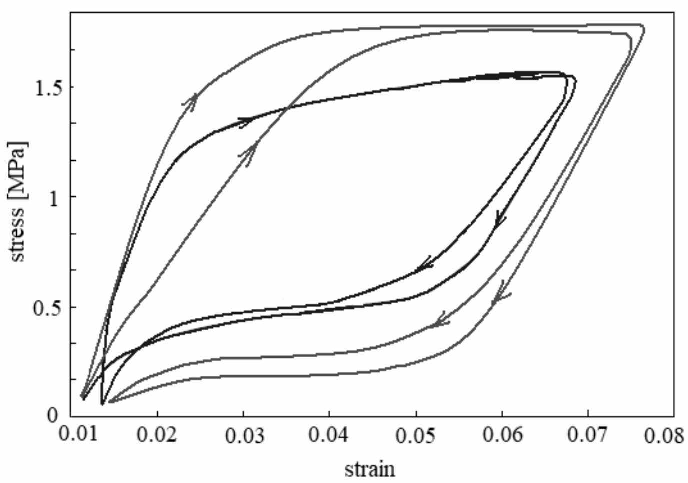

Fig. 8 – The progressive enhancement of the stiffness.

5. CONCLUSIONS

To sum up, this paper focuses on a soft robot obtained by folding an elastomer foil with embedding the artificial muscles made from shape memory alloys. The robot is designed to provide the motion observed in the human arm, for example for drug delivery and minimally-invasive surgical procedures [22, 23]. Examples of different approaches in this subject can be found in [24–27]. The robot contains an elastic central column connected between the platforms capable to produce angular displacements between the platforms. The actuation and force characteristics are investigated by using a Book-Wen model coupled to the intrinsic time measure of the temperature which governs the behavior of the SMAs.

Acknowledgements. This work was supported by a grant of the Romanian ministry of Research and Innovation, CCCDI – UEFISCDI, project number PN–III–P1–1.2–PCCDI–2017–0221/ 59PCCDI/2018 (IMPROVE), within PNCDI III.

Received on January 5, 2020

REFERENCES

1. MAJIDI, C., Soft *Robotics: A Perspective - Current Trends and Prospects for the Future*, Soft Robotics, **1**, *1*, pp. 5–11, 2013; doi: 10.1089/soro.2013.0001.
2. RUS, D., TOLLEY, M., *Design, fabrication and control of soft robots*, Nature **521**, pp. 467–475, 2015.
3. SCHMITT, F., PICCIN, O., BARBÉ, L., BAYLE, B., *Soft Robots Manufacturing*: *A Review*, Front. Robot., AI 5:84, 2018; https://doi.org/10.3389/frobt.2018.00084.

4. MAHADEVAN, L., RICA, S., *Self-organized origami*, Science, **307**, *5716*, p. 1740, 2005; doi: 10.1126/science.1105169.
5. LEE, D.Y., KIM, S.R., KIM, J.S., PARK, J.J., CHO, K.J, *Origami wheel transformer: a variable-diameter wheel drive robot using an origami structure*, Soft Robotics, **4**, *2*, pp. 163–180, 2017; doi: 10.1089/soro.2016.0038.
6. TUMER, N., GOODWINE, B., SEN, M., *A review of origami applications in mechanical engineering*, Proc. Inst. Mech. Eng., Part C, **230**, *14*, pp. 2345–2362, 2016; doi.org/10.1177/0954406215597713.
7. ROURKE, O.J., *How to Fold It: The Mathematics of Linkages, Origami, and Polyhedra*, Cambridge Univ. Press, 2011.
8. LANG, R.J., *Twists, Tilings, and Tesselations. Mathematical Methods for Geometric Origami*, CRC Press, 2017.
9. LUO, M., YAN, R., WAN, Z., QIN, Y., SANTOSO, J., SKORINA, E.H., ONAL, C.D., *OriSnake: Design, Fabrication, and Experimental Analysis of a 3-D Origami Snake Robot*, IEEE Robotics and Automation Letters, **3**, *3*, pp. 1993–1999, 2007.
10. LASCHI, C., MAZZOLAI, B., CIANCHETTI, M., *Soft robotics: technologies and systems pushing the boundaries of robot abilities*, Sci. Robot., **1**, *1*, 2016; doi:10.1126/scirobotics. aah3690.
11. BRIŞAN, C., BOANTĂ, C., CHIROIU, V., *Introduction in optimization of industrial robots. Theory and applications*, Edit. Academiei Române, 2019.
12. MAZZOLAI, B., MARGHERI, L., CIANCHETTI, M., DARIO, P., LASCHI, C., *Soft-robotic arm inspired by the octopus: II. From artificial requirements to innovative technological solutions*, Bioinspir. Biomim., **7**, *2*, 2012; doi: 10.1088/1748-3182/7/2/025005.
13. KURIBAYASHI, K., *Millimeter-sized joint actuator using a shape memory alloy*, Sensors and Actuators, **20**, *1–2*, pp. 57–64, 1989.
14. TANIGUCHI, H., *Flexible artificial muscle actuator using coiled shape memory alloy wires*, APCEE Procediu **7**, pp. 54–50, 2013.
15. VERHOEVEN, R., HILLER, M., TADOKORO, S., *Workspace of tendon-driven Stewart platforms: Basics, classification, details on the planar 2-DOF class*, International Conference on Motion and Vibration Control MOVIC, Institute of Robotics, Zürich, Switzerland, **3**, pp. 871–876, 1998.
16. SIMAAN, N., SHOHAM, M., *Geometric interpretation of the derivatives of parallel robots' Jacobian matrix with application to stiffness control*, Journal of Mechanical Design, **125**, *1*, pp. 33–42, 2003.
17. HAY, A.M., SNYMAN, J.A., *The chord method for the determination of nonconvex workspaces of planar parallel manipulators*, Computers & Mathematics with Applications, **43**, *8*, pp. 1135–1151, 2002.
18. KHAN, R., BILLAH, M, WATENABE, M., SHAFIE, A.A., *Small Scale Parallel Manipulator Kinematics for Flexible Snake Robot Application*, Communications in Control Science and Engineering (CCSE), **2**, pp. 82–87, 2014.
19. CHIROIU, V., IONESCU, M.F., SIRETEANU, T., IOAN, R., MUNTEANU, L., *On intrinsic time measure in the modeling of cyclic behavior of a Nitinol cubic block*, Smart Materials and Structures, **24**, *3*, 035022, pp. 1–11, 2015.
20. KADASHEVICH, Y.I., MOSOLOV, A.B., *Endochronic theory of plasticity: Fundamentals and outlook,* Izvestiia Akademii Nauk SSSR, Mekhanika Tverdogo Tela, **1**, pp. 161–168, 1989.
21. BOUC, R., *Modèle mathématique d'hystérésis*, Acustica, **24**, pp. 16–25, 1971.
22. BIRLESCU, I., HUSTY, M., VAIDA, C., PLITEA, N., NAYAK, A., PÎSLĂ, D., *Complete Geometric Analysis Using the Study SE(3) Parameters for a Novel, Minimally Invasive Robot Used in Liver Cancer Treatment,* Symmetry, **11**, *12*, 1491, 2019.
23. PÎSLĂ, D., BIRLESCU, I., VAIDA, C., TUCAN, P., PÎSLĂ, A., GHERMAN, B., CRIŞAN, N., PLITEA, N., *Algebraic Modeling of Kinematics and Singularities for a Prostate Biopsy Parallel Robot*, Proceedings of the Romanian Academy, series A: Mathematics, Physics, Technical Sciences, Information Science, **19**, *3*, pp. 489–497, 2018.

24. CHIROIU, V., MUNTEANU, L., RUGINĂ, C., *On the control of a cooperatively robotic system by using a hybrid logic algorithm*, Proceedings of the Romanian Academy, series A: Mathematics, Physics, Technical Sciences, Information Science, **19**, *4*, pp. 589–596, 2018.
25. PLITEA, N., SZILAGHYI, A., PÎSLĂ, D., *Kinematic Analysis of a new 5-DOF Modular Parallel Robot for Brachytherapy*, Robotics and Computer Integrated Manufacturing, **31**, pp. 70–80, 2015; doi.org/10.1016/j.rcim.2014.07.005.
26. MUNTEANU, L., RUGINĂ, C., DRAGNE, C., CHIROIU, V., *On the Robotic Control Based on Interactive Activities of Subjects*, Proceedings of the Romanian Academy, series A: Mathematics, Physics, Technical Sciences, Information Science (in press).
27. CHIROIU, V., MUNTEANU, L., IOAN, R., DRAGNE, C., MAJERCSIK, L., *Using the Sonification for Hardly Detectable Details in Medical Images*, Scientific Reports, 9, article number 17711, 2019; https://doi.org/10.1038/s41598–019–54080–7.